

A ROBUST STABLE PI CONTROLLER DESIGN IN TIME-FREQUENCY DUAL DOMAINS FOR AIRCRAFT ENGINE

Nan Liu*

*Shanghai Aircraft Design & Research Institute, Commercial Aircraft Corp. of China,
Shanghai, China, 201210

Keywords: Aircraft Engine, interval system, D-decomposition, PI control, robust stable

Abstract

For the parameters uncertainty of aircraft engine brought by nonlinearity or unit difference, an optimal PI controller with robust stability design method in time-frequency dual domains is proposed. Interval system is decomposed into several vertex sub-systems using boundary principle. D-decomposition technology and graphic approach of PI parameters stability region with specified gain and phase margins are integrated to construct the stability boundaries of sub-systems. The PI parameters robust stability region of interval system satisfying the specified gain and phase margins is obtained using the boundaries. The optimal PI controller is calculated in this region with the object of dynamic performance and robustness. The developed method is applied to the aircraft engine, and the simulation results of high pressure spool rotational speed loop and turbine pressure ratio loop validate the high control quality, and the robustness is also tested.

1 Introduction

In industrial practice, it is usually difficult to describe the plant accurately in a control system. There always exist some uncertain factors in the established system model. For aircraft engines, there are many uncertain factors for the representation of dynamic, which suffer from modeling errors, nonlinearities, and unit difference and so on. Because of these, aircraft engine becomes an interval system with parameters uncertainty. It is impossible to keep the performance quality and system stability for the controller designed from the system with

certain fixed parameters. Due to above uncertainties, robust control of aircraft engine has been an important problem for the developer. Now, there are a lot of robust control method applied to aircraft engine, such as LQG/LTR algorithm [1], H_∞ method [2], and LPV approach [3]. However, these robust algorithms could not establish a direct visualized robust stability region of control parameters, and it could not ensure the system satisfy the stability margin targets. For the robust control problem of interval system, it is usually transformed to the stability problem of characteristic polynomial when the coefficients are subject to some perturbations. Kharitonov theorem is a significant result in the field of robust stability systems with uncertain parameters. It addresses how to analyze the Hurwitz stability of the interval system through a finite subset of vertical polynomials, which is known as Kharitonov polynomials. It succeeds in reducing the computational burden required in determining the stability of such polynomial families [4, 5]. Edge theorem develops the one dimension examination of stability for the family of polynomials with affine linear uncertainty structure. It points out that the coefficients are not independent in the case of interval polynomials [6, 7]. Generalized Kharitonov theory proved that the required edge number of edge theorem is dependent on the number of polynomials not on the number of uncertain parameters [8]. These two theorems have been proved based on the zero exclusion principle [9] and the value set concept [10]. However, these classic approaches only consider the stability, and ignore the dynamic

performance requirement and stability margin in frequency domain. In this paper, a new robust stable optimal PI controller design method in time-frequency dual frequency domain is proposed, which could make the system satisfy the specified gain and phase margin. This approach transforms the interval system to vertical sub-systems based on the edge theorem and bounds principle. Combining the graphics method of PI controller with gain and phase margin specifications, the D-decomposition [11] technology is employed to establish the robust stable region of PI parameters for the interval system with specified gain and phase margin. According to the performance request, the optimal PI control parameters are searched out in the region of robust stability. Finally, nonlinear model simulations of aircraft engine validate the effectiveness of the proposed method.

2 PI Control System of Interval Parameters with Time Delay

Consider the following PI feedback control system with time delay as Fig. 1. In the figure, $r(t)$ is input, $y(t)$ is output.

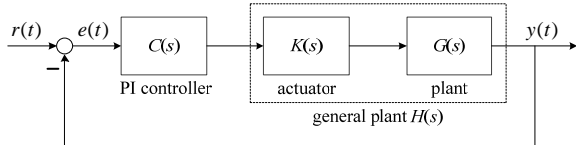


Fig. 1 PI Control System with Time Delay

$G(s)$ is the plant with interval parameters

$$G(s) = \frac{B_1(s)}{A_1(s)} \quad (1)$$

$K(s)$ is the actuator with time delay

$$K(s) = \frac{B_2(s)}{A_2(s)} e^{-Ls} \quad (2)$$

$C(s)$ is the PI controller

$$C(s) = k_p + \frac{k_I}{s} \quad (3)$$

The general plant $H(s)$ is composed of $G(s)$ and $K(s)$ and it is represented as

$$\begin{aligned} H(s) &= G(s)K(s) = \frac{B(s)}{A(s)} = \frac{B_1(s)B_2(s)}{A_1(s)A_2(s)} e^{-Ls} \\ &= \frac{b_m s^m + b_{m-1} s^{m-1} + \dots + b_1 s + b_0}{a_n s^n + a_{n-1} s^{n-1} + \dots + a_1 s + a_0} e^{-Ls} = \frac{\sum_{j=0}^m b_j s^j}{\sum_{i=0}^n a_i s^i} e^{-Ls} \end{aligned} \quad (4)$$

where, L is time delay, $a_i \in [\underline{a}_i, \bar{a}_i]$, $i = 0, 1, \dots, n$, $b_j \in [\underline{b}_j, \bar{b}_j]$, $j = 0, 1, \dots, m$, $n \geq m$, $a_n \neq 0$. a_i and b_j are interval parameters.

For such a closed-loop system in Fig. 1, the characteristic polynomial is transcendental because of the delay and uncertain parameters, and it could be described using the following quasi-polynomial family

$$\begin{aligned} P(s; k_p, k_I) &= s(a_n s^n + a_{n-1} s^{n-1} + \dots + a_1 s + a_0) + \\ &+ (k_p s + k_I)(b_m s^m + b_{m-1} s^{m-1} + \dots + b_1 s + b_0) e^{-Ls} \quad (5) \\ &= s \sum_{i=0}^n a_i s^i + (k_p s + k_I) \sum_{j=0}^m b_j s^j e^{-Ls} \end{aligned}$$

Based on the boundary theory [6], there are interval parameters in Equ.4 and it could be converted to vertical sub-systems.

$$\begin{aligned} H_1(s) &= \frac{\underline{b}_m s^m + \underline{b}_{m-1} s^{m-1} + \dots + \underline{b}_1 s + \underline{b}_0}{\underline{a}_n s^n + \underline{a}_{n-1} s^{n-1} + \dots + \underline{a}_1 s + \underline{a}_0} e^{-Ls} \\ &\vdots \\ H_i(s) &= \frac{\hat{b}_m s^m + \hat{b}_{m-1} s^{m-1} + \dots + \hat{b}_1 s + \hat{b}_0}{\hat{a}_n s^n + \hat{a}_{n-1} s^{n-1} + \dots + \hat{a}_1 s + \hat{a}_0} e^{-Ls} \quad (6) \\ &\vdots \end{aligned}$$

$$H_{2^{n+m+2}}(s) = \frac{\bar{b}_m s^m + \bar{b}_{m-1} s^{m-1} + \dots + \bar{b}_1 s + \bar{b}_0}{\bar{a}_n s^n + \bar{a}_{n-1} s^{n-1} + \dots + \bar{a}_1 s + \bar{a}_0} e^{-Ls}$$

The corresponding characteristic polynomials are

$$\begin{aligned} P_1(s; k_p, k_I) &= s(\underline{a}_n s^n + \underline{a}_{n-1} s^{n-1} + \dots + \underline{a}_1 s + \underline{a}_0) \\ &+ (k_p s + k_I)(\underline{b}_m s^m + \underline{b}_{m-1} s^{m-1} + \dots + \underline{b}_1 s + \underline{b}_0) e^{-Ls} \\ &\vdots \\ P_i(s; k_p, k_I) &= s(\hat{a}_n s^n + \hat{a}_{n-1} s^{n-1} + \dots + \hat{a}_1 s + \hat{a}_0) \\ &+ (k_p s + k_I)(\hat{b}_m s^m + \hat{b}_{m-1} s^{m-1} + \dots + \hat{b}_1 s + \hat{b}_0) e^{-Ls} \quad (7) \\ &\vdots \\ P_{2^{n+m+2}}(s; k_p, k_I) &= s(\bar{a}_n s^n + \bar{a}_{n-1} s^{n-1} + \dots + \bar{a}_1 s + \bar{a}_0) \\ &+ (k_p s + k_I)(\bar{b}_m s^m + \bar{b}_{m-1} s^{m-1} + \dots + \bar{b}_1 s + \bar{b}_0) e^{-Ls} \end{aligned}$$

3 Robust Stability Region of PI Parameters for Interval System with Time Delay

The corresponding convex polytope composed of the quasi-polynomial family in Equ.7 would have 2^{n+m+2} vertexes.

$$R = \text{conv} \{P_1, P_2, \dots, P_{2^{n+m+2}}\} \quad (8)$$

where, conv denote generating convexly, and the first items of $P_i(s; k_p, k_I)$ must be the same sign.

Definition 1 [12], Given a set D in the complex plane, the delay system of Equ.4 is called D-stable if the zeros of the characteristic quasi-polynomial $P(s; k_p, k_I)$ in Equ.5 stay in D. If so, $P(s; k_p, k_I)$ is called D-stable. In particular, $P(s; k_p, k_I)$ is called stable $P(s; k_p, k_I)$ is D-stable for D being the open left-half plane.

Theorem 1, For the interval quasi-polynomial family $H(s)$, one PI controller could ensure the stability of the whole interval quasi-polynomial family, if and only if this PI controller could ensure the stability of every vertical sub-system $H_i(s) \in H(s)$.

Proof: For the interval system of Fig.1, the open loop transfer function including the vertical subsystem $H_i(s)$ is represented as

$$T_i(s) = C(s)H_i(s) = \frac{q_i(s)}{p_i(s)}, i = 1, 2, \dots, 2^{m+n+2} \quad (9)$$

The polytope composed of characteristic quasi-polynomial family of the unit feedback system with interval parameters is

$$R_T = \text{conv} \{(T_1(s) + 1)p_1(s), (T_2(s) + 1)p_2(s), \dots, (T_{2^{m+n+2}}(s) + 1)p_{2^{m+n+2}}(s)\} \quad (10)$$

In Definition 1, let D be the open left-half plane, according to the edge theorem, the system with uncertainty $H(s)$ would be stable if every edge $(T_i(s) + 1)p_i(s)$ of the polytope R_T is D-stable. It is worth noting that $(T_i(s) + 1)p_i(s)$ is the closed-loop characteristic polynomial of sub-system $H_i(s)$, so the stability of $(T_i(s) + 1)p_i(s)$ is equivalent to the stability of $H_i(s)$. End

From Theory 1, the PI parameters' robust stability region of $H(s)$ would be the intersection of all sub-systems.

Define the PI parameters range of vertical sub-system $H_i(s)$

$$Q = \{k_p \in [-\infty, \infty], k_I \in [-\infty, \infty]\} \quad (11)$$

If parameters' stability region of closed-loop characteristic polynomial for $H_i(s)$ is S_i , then $S_i \in Q$. The stability region of $H(s)$ would be

$$S = S_1 \cap S_2 \cap \dots \cap S_{2^{n+m+2}} \quad (12)$$

Based on D-decomposition method [11], the stability region of controller parameters can be determined by the union of hyper-surfaces

$$\begin{cases} \partial D_0 = \{(k_p, k_I) \in Q; P_i(0; k_p, k_I) = 0\} \\ \partial D_\infty = \{(k_p, k_I) \in Q; P_i(\infty; k_p, k_I) = 0\} \\ \partial D_\omega = \{(k_p, k_I) \in Q; P_i(j\omega; k_p, k_I) = 0, \\ \forall \omega \in (-\infty, 0) \cup (0, \infty)\} \end{cases} \quad (13)$$

Where, ∂D_0 is real root boundary (RRB), ∂D_∞ is infinite root boundary (IRB), ∂D_ω is complex root boundary (CRB). The whole boundary $\partial D = \partial D_0 \cup \partial D_\infty \cup \partial D_\omega$.

The three boundaries could be calculated separately for $P_i(s; k_p, k_I)$.

(1) real root boundary ∂D_0

For characteristic polynomial of $P_i(s; k_p, k_I)$, ∂D_0 is computed as

$$P_i(0; k_p, k_I) = \hat{b}_0 k_I = 0 \Rightarrow k_I = 0 \quad (14)$$

(2) Infinite root boundary ∂D_∞

Because of time delay, the characteristic polynomial of $P_i(s; k_p, k_I)$ would have infinite number roots which cannot be calculated analytically in the general case. According the paper of [13], ∂D_∞ could be calculated as

$$\begin{cases} k_p = -\frac{\hat{a}_n}{\hat{b}_m} & n = m \\ \text{none} & n > m \end{cases} \quad (15)$$

(3) Complex Root Boundary ∂D_ω

Rewrite the closed-loop characteristic polynomial of $H_i(s)$ as

$$P_i(s; k_p, k_I) = sA_i(s) + (k_p s + k_I)B_i(s)e^{-Ls} \quad (16)$$

Let $P_i^*(s; k_p, k_I) = P_i(s; k_p, k_I)e^{Ls}$, then $P_i^*(s; k_p, k_I)$ would be

$$P_i^*(s; k_p, k_I) = sA_i(s)e^{Ls} + (k_p s + k_I)B_i(s) \quad (17)$$

Since Ls has no zeros, the stability regions of Equ. 16 and 17 are equivalent. Substitute $s = j\omega$ to Equ.16, and select the range of ω is because of symmetry [13], Equ.17 can be rewritten as

$$P_i^*(j\omega; k_p, k_I) = j\omega(A_{iR} + jA_{iI})e^{jL\omega} + (jk_p\omega + k_I)(B_{iR} + jB_{iI}) \quad (18)$$

where

$$\begin{cases} A_{iR} = A_{i1R}A_{i2R} - A_{i1I}A_{i2I} \\ A_{iI} = A_{i1R}A_{i2I} + A_{i1I}A_{i2R} \\ B_{iR} = B_{i1R}B_{i2R} - B_{i1I}B_{i2I} \\ B_{iI} = B_{i1R}B_{i2I} + B_{i1I}B_{i2R} \end{cases}$$

Subscript R denotes the real part and I denotes the image part. Substitute the Euler formula $e^{jL\omega} = \cos(L\omega) + j\sin(L\omega)$ to Equ.17, and separate $P_i^*(s; k_p, k_I)$ into real and image parts where,

$$\begin{cases} P_{iR}(\omega; k_p, k_I) = -A_{iI}\omega\cos(L\omega) - A_{iR}\omega\sin(L\omega) - k_p B_{iI}\omega + k_I B_{iR} \\ P_{iI}(\omega; k_p, k_I) = -A_{iI}\omega\sin(L\omega) + A_{iR}\omega\cos(L\omega) + k_p B_{iR}\omega + k_I B_{iI} \end{cases} \quad (19)$$

It can be found from Equ.19 that $P_{iR}(\omega; k_p, k_I)$ and $P_{iI}(\omega; k_p, k_I)$ are continuous functions of k_p and k_I , and the stability region of Equ.17 is a subset of Q .

According to implicit function existence theorem, if the Jacobian matrix of Equ.20 is nonsingular, then the only solution curve $(k_p(\omega), k_I(\omega))$ about ω could be calculated from the equations of Equ.21.

$$J = \begin{bmatrix} \frac{\partial P_{iR}}{\partial k_p} & \frac{\partial P_{iR}}{\partial k_I} \\ \frac{\partial P_{iI}}{\partial k_p} & \frac{\partial P_{iI}}{\partial k_I} \end{bmatrix}_{(\omega; k_p, k_I)} \quad (20)$$

$$\begin{cases} P_{iR}(\omega; k_p, k_I) = 0 \\ P_{iI}(\omega; k_p, k_I) = 0 \end{cases} \quad (21)$$

Lemma 1 [14], Along the direction of ω increasing, if $\det J < 0$, the parameters stability region locates the right hand side of curve $(k_p(\omega), k_I(\omega))$; if $\det J > 0$, the parameters

stability region locates the left hand side of curve $(k_p(\omega), k_I(\omega))$.

Equ.21 can be rewritten as a function of ω .

$$\begin{cases} k_p = \frac{-B_{iI}X(\omega) + B_{iR}Y(\omega)}{B_{iR}^2 + B_{iI}^2} \\ k_I = \frac{B_{iI}Y(\omega) + B_{iR}X(\omega)}{B_{iR}^2 + B_{iI}^2} \omega \end{cases} \quad (22)$$

where,

$$\begin{cases} X(\omega) = A_{iI}\cos(L\omega) + A_{iR}\sin(L\omega) \\ Y(\omega) = A_{iI}\sin(L\omega) - A_{iR}\cos(L\omega) \end{cases} \quad (22)$$

From Equ. 22, it can be found that when ω changes, a parameters curve $(k_p(\omega), k_I(\omega))$ can be drawn in the plane of $k_p - k_I$. This curve is the complex root boundary ∂D_ω .

From Equ.19 and 20, the Jacobian matrix is computed as

$$J = \begin{bmatrix} -B_{iI}\omega & B_{iR} \\ B_{iR}\omega & B_{iI} \end{bmatrix} \quad (23)$$

The following is obvious.

$$\det J = -\omega(B_{iR}^2 + B_{iI}^2) < 0, \omega \in (0, +\infty) \quad (24)$$

Based on the Lemma 1, along the direction of ω increasing, the parameters stability region locates the right hand side of the parameters curve.

4 Stability region with gain and phase margin specifications

For a control system, stability is a basic design requirement. Besides this, the system usually should satisfy gain and phase margin specifications in frequency domain [15, 16]. So the stability region with specific gain margin h and phase margin γ would be developed deeper in this paper.

Since the definition of gain and phase margin

$$\frac{(jk_p\omega_{ix} + k_I)(B_{iR} + jB_{iI})}{j\omega_{ix}(A_{iR} + jA_{iI})}e^{-jL\omega_{ix}} = -\frac{1}{h} \quad (25)$$

$$\frac{(jk_p\omega_{ic} + k_I)(B_{iR} + jB_{iI})}{j\omega_{ic}(A_{iR} + jA_{iI})}e^{-jL\omega_{ic}} = -e^{j\gamma} \quad (26)$$

They could be rewritten as

$$j\omega_{ix}(A_{iR} + jA_{iI})e^{jL\omega_{ix}} + h(jk_p\omega_{ix} + k_I)(B_{iR} + jB_{iI}) = 0 \quad (27)$$

$$j\omega_{ic}(A_{iR} + jA_{iI})e^{j(L\omega_{ic} + \gamma)} + (jk_p\omega_{ic} + k_I)(B_{iR} + jB_{iI}) = 0 \quad (28)$$

where, ω_{ix} is phase crossover frequency of $C_i(j\omega)H_i(j\omega)$, and ω_{ic} is the gain crossover frequency of $C_i(j\omega)H_i(j\omega)$.

Compare Equ.18 with Equ.27 and 28, there exist the only difference about h and γ . The new representation could be obtained for the gain and phase margin specifications through the similar derivation.

$$\begin{cases} k_{ph} = \frac{-B_{il}X_h(\omega) + B_{ir}Y_h(\omega)}{h(B_{ir}^2 + B_{il}^2)} \\ k_{ih} = \frac{B_{il}Y_h(\omega) + B_{ir}X_h(\omega)}{h(B_{ir}^2 + B_{il}^2)}\omega \end{cases} \quad (29)$$

where

$$\begin{cases} X_h(\omega) = A_{il} \cos(L\omega) + A_{ir} \sin(L\omega) \\ Y_h(\omega) = A_{il} \sin(L\omega) - A_{ir} \cos(L\omega) \end{cases}$$

$$\begin{cases} k_{p\gamma} = \frac{-B_{il}X_\gamma(\omega) + B_{ir}Y_\gamma(\omega)}{B_{ir}^2 + B_{il}^2} \\ k_{i\gamma} = \frac{B_{il}Y_\gamma(\omega) + B_{ir}X_\gamma(\omega)}{B_{ir}^2 + B_{il}^2}\omega \end{cases} \quad (30)$$

where

$$\begin{cases} X_\gamma(\omega) = A_{il} \cos(L\omega + \gamma) + A_{ir} \sin(L\omega + \gamma) \\ Y_\gamma(\omega) = A_{il} \sin(L\omega + \gamma) - A_{ir} \cos(L\omega + \gamma) \end{cases}$$

For the parameters region of satisfying gain and margin, we have

$$\det J_h = -\omega h^2 (B_{ir}^2 + B_{il}^2) < 0, \omega \in (0, +\infty) \quad (31)$$

$$\det J_\gamma = -\omega (B_{ir}^2 + B_{il}^2) < 0, \omega \in (0, +\infty) \quad (32)$$

The complex root boundaries with gain and phase margins specifications could be plotted separately based on Equ.29 and 30. Along the direction of ω increasing, the stability regions locate the right hand side of the boundary curves. The intersection of these regions is the PI parameters stability region being satisfy gain margin and phase margin at the same time.

The PI parameters stability region S_i of $H_i(s)$ could be established from ∂D_0 , ∂D_∞ and ∂D_ω . The whole stability region S of interval quasi-polynomial could be calculated from Equ.12.

5 Optimization of PI Parameters

Stability is only a basic quality for control system. Although all sets of (k_p, k_i) in the

region S could stabilize $H(s)$, the dynamic performance would be different. Besides stability, tacking performance and rejection capacity should be also considered for the controller's design. In this paper, the evaluation function of control quality is defined as follows

$$f(k_p, k_i) = \lambda_1 \sigma + \lambda_2 t_s + \lambda_3 M_s, \lambda_1 + \lambda_2 + \lambda_3 = 1 \quad (33)$$

where, overshoot σ and settling time t_s mean the tracking performance, and sensitivity M_s means rejection capacity. λ_1 , λ_2 , λ_3 are weights coefficients and could be selected based the request of control quality.

Then an optimal problem about seeking of (k_p, k_i) in S is established.

$$\begin{cases} \min(f(k_p, k_i)) \\ s.t. (k_p, k_i) \in S \end{cases} \quad (34)$$

The solution of Equ.34 is the optimal PI parameters. Here, a traversal seeking strategy is employed to solve the optimal problem.

6 Robust PI Control of Aircraft Engine

In this paper, the component nonlinear model of aircraft engine is selected as the plant. Since the strong nonlinearity of its dynamic, it is impossible to design the controller directly. Usually, the corresponding linear models are established at different flight conditions, and then the controllers are designed for the linear models separately. The intermediate rating linear model of high pressure spool rotational speed loop at altitude $H = 0$ m, Mach number $Ma = 1.0$ is

$$G_{N_H}(s) = \frac{0.3268s + 1.335}{s^2 + 10.72s + 28.1} \quad (35)$$

The actuator of fuel flow is

$$K_{N_H}(s) = \frac{1}{0.116s + 1} e^{-0.04s} \quad (36)$$

The general plant of high pressure spool rotational speed loop is

$$\begin{aligned} H_{N_H}(s) &= K_{N_H}(s)G_{N_H}(s) \\ &= \frac{0.3268s + 1.335}{(0.116s + 1)(s^2 + 10.72s + 28.1)} e^{-0.04s} \end{aligned} \quad (37)$$

In a small neighborhood around above operation point, four sub-systems are obtained

$$H_{N_H1}(s) = \frac{0.2614s + 1.084}{(0.116s + 1)(s^2 + 8.576s + 22.48)} e^{-0.04s} \quad (38a)$$

$$H_{N_H2}(s) = \frac{0.2614s + 1.084}{(0.116s + 1)(s^2 + 12.864s + 33.72)} e^{-0.04s} \quad (38b)$$

$$H_{N_H3}(s) = \frac{0.3922s + 1.602}{(0.116s + 1)(s^2 + 8.576s + 22.48)} e^{-0.04s} \quad (38c)$$

$$H_{N_H4}(s) = \frac{0.3922s + 1.602}{(0.116s + 1)(s^2 + 12.864s + 33.72)} e^{-0.04s} \quad (38d)$$

According to the method in Section 3, the PI parameters stability regions of these four vertical sub-systems are shown in Fig.2 using D-decomposition technology. In particular, for high pressure spool rotational speed loop of aircraft engine, $n=3$ $m=2$, $n > m$, infinite root boundary is not exist. The shadow in Fig.2 is the intersection of stability regions of vertical sub-systems, and this region is just S . If the specified gain and phase margin is given as $(h, \gamma) = (16.9\text{dB}, 65^\circ)$, the new PI parameters stability region is shown as in Fig.3.

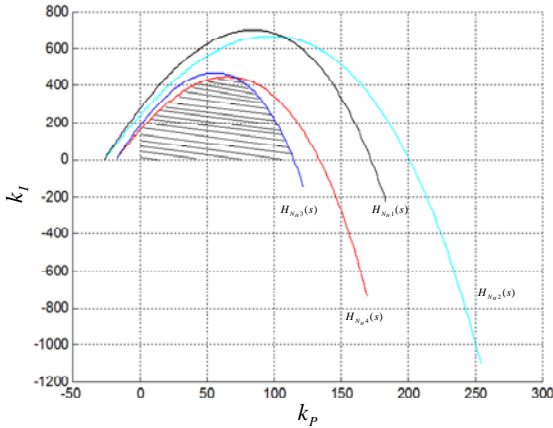


Fig. 2 PI Parameters Stability Regions of Vertical Systems

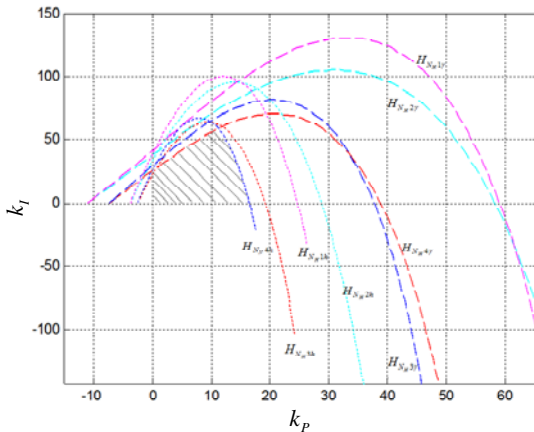


Fig. 3 PI Parameters Stability Regions of Vertical Systems

Solve the optimization problem of Equ.34 in shadow region of Fig.3, and the optimal PI parameters are calculated as $(k_p, k_I) = (11.5, 53.5)$. The simulation results of its effect on the aircraft engine nonlinear model are show in Fig.4. From the results in Fig.4, it is obvious that the vertical sub-systems are all stable. $H_{N_H4}(s)$ has the maximum overshoot, not more than 1.75%; $H_{N_H1}(s)$ has the longest settling time, not longer than 1.36s. In order to verify the effect of the interval system with the computed PI controller, the following four sub-systems Equ.39a-39d are chosen to simulate and the results are shown in Fig.5. The four sub-systems are all stable, and the responses have no overshoot. The longest settling time is $H_{N_H5}(s)$, only 1.3s.

$$H_{N_H5}(s) = \frac{0.2614s + 1.084}{(0.116s + 1)(s^2 + 10.72s + 28.1)} e^{-0.04s} \quad (39a)$$

$$H_{N_H6}(s) = \frac{0.3922s + 1.602}{(0.116s + 1)(s^2 + 10.72s + 28.1)} e^{-0.04s} \quad (39b)$$

$$H_{N_H3}(s) = \frac{0.3268s + 1.335}{(0.116s + 1)(s^2 + 8.576s + 22.48)} e^{-0.04s} \quad (39c)$$

$$H_{N_H4}(s) = \frac{0.3268s + 1.335}{(0.116s + 1)(s^2 + 12.864s + 33.72)} e^{-0.04s} \quad (39d)$$

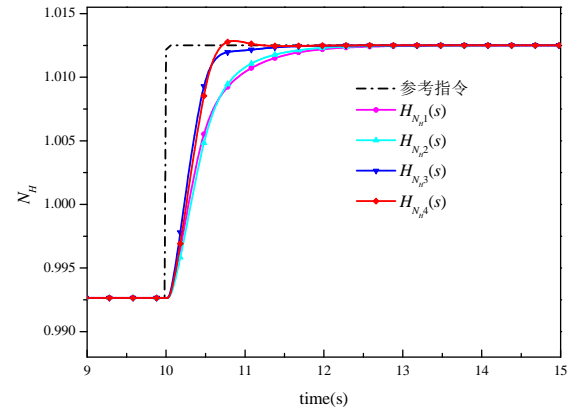


Fig. 4 Responses of Vertical Sub-Systems for High Pressure Spool Rotational Speed Loop

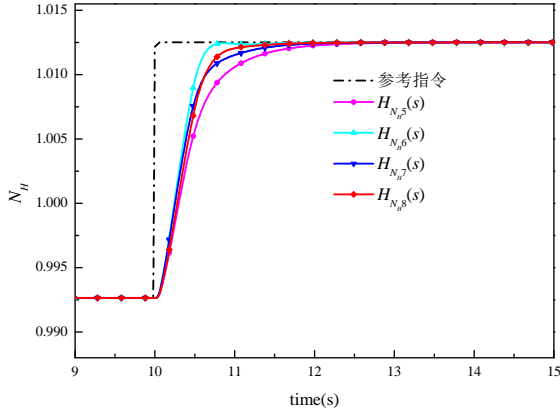


Fig. 5 Responses of Interval System for High Pressure Spool Rotational Speed Loop

At above flight condition, altitude $H = 0$ m, Mach number $Ma = 1.0$, the intermediate rating linear model of turbine pressure ratio loop and the actuator are

$$G_{\pi_i}(s) = \frac{11.32s + 158 + 490.4}{s^2 + 15.77s + 58.69} \quad (40)$$

$$K_{\pi_i}(s) = \frac{1}{0.02s + 1} e^{-0.02s} \quad (41)$$

In the small neighborhood of this operation point, four vertical sub-systems are also could be established. The optimal PI parameters is computed as $(k_p, k_i) = (0.02, 1.1)$, and the step response of vertical sub-systems and validation simulations are shown in Fig.6 and 7 separately. In Fig.6, all the vertical subsystems are stable and have no overshoot. $H_{\pi_1}(s)$ has the longest settling time, no longer than 0.4s. In Fig.7, the sub-systems to be validated are also stable, and have no overshoot. $H_{\pi_5}(s)$ has the longest settling time, no longer than 0.4s.

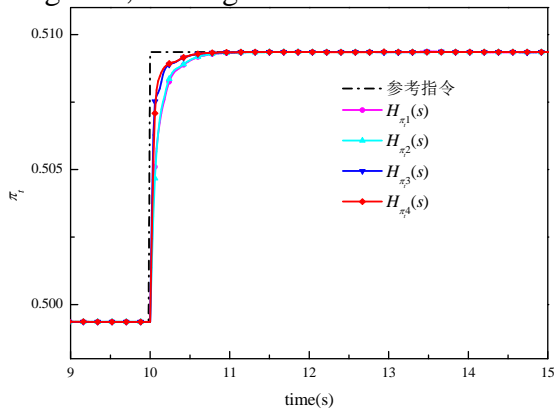


Fig. 6 Step Responses of Vertical Sub-systems of Turbine Pressure Ratio Loop

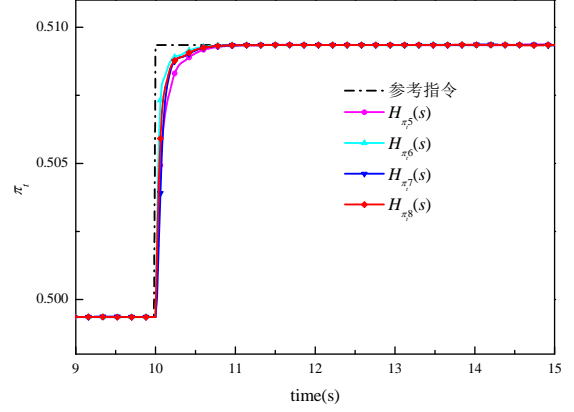


Fig. 7 Step Response of Interval System of Turbine Pressure Ratio Loop

7 Conclusions

In this paper, a robust stability optimal PI controller design method with gain and phase margin specifications in time-frequency dual domain is proposed. This approach decomposes the robust stability problem of interval system into vertical sub-systems. And combine D-decomposition technology and graphic tuning method of PI parameters to establish the PI parameters robust stability region of interval system with gain and phase margin specifications, and calculate the optimal solution in this region. The simulations on the nonlinear model of aircraft engine validate the effectiveness of optimal PI controller under the uncertainty and the keeping ideal control quality.

Reference

- [1] Soeder James F. F100 multivariable control synthesis program-computer implementation of the F100 multivariable control algorithm. NASA-2231, 1983.
- [2] Samar Raza, Postlethwaite Ian. Design and implementation of a digital multimode H-infinity controller for the Spey turbofan engine. *Journal of Dynamic System Measurement and Control*, Vol. 132, No. 1, 011010, 2010.
- [3] Gilbert Wilfried, Henrion Didier, Bemussou Jacques. Polynomial LPV synthesis applied to turbofan engines. *Control Engineering Practice*, Vol. 18, No. 9, pp 1077-1083, 2010.
- [4] Kharitonov V L. Asymptotic stability of an equilibrium position of a family of systems of linear differential equations. *Differential Equations*, Vol 14, No 1, pp 1483-1485, 1979.
- [5] Auba T, Funahashi Y. A note on Kharitonov's theorem, *IEEE Transactions on Automatic Control*, Vol. 38, No. 4, pp 663-664, 1993.

- [6] Bartlett A C, Holot C V, Huang Lin. Root location of an entire polytope of polynomials: it suffices to check the edges. *Math Control Signals Systems*, Vol. 1, No.1, pp 61-71, 1988.
- [7] Wang Long, Wang Zhizhen, Wenshen Yu, et al. Edge theorem for MIMO systems. *IEEE Transactions on Circuits and Systems—I: Fundamental Theory and Applications*, Vol. 50, No. 12, pp 1577-1580, 2003.
- [8] Chapellat H, Bhattacharyya S P. A generalization of Kharitonov's theorem: robust stability of interval plants. *IEEE Transactions on Automatic Control*, Vol. 34, No. 3, pp 306-311, 1989.
- [9] Ramirez-Sosa M M I, Torres-Munoz J A, Kharitonov V L. On multivariable zero exclusion principle: application to stability radius. *Proceedings of the 38th IEEE Conference on Decision and Control*, Phoenix, Vol. AZ, pp 4531- 4536, 1999.
- [10] Moornani K A, Haeri M. Robust stability testing function and Kharitonov-like theorem for fractional order interval systems. *IET Control Theory and Applications*, Vol. 4, No. 10, pp 2097-2109, 2010.
- [11] Gryazina Elena N, Polyak Boris T. Stability regions in the parameter space: D-decomposition revisited, *Automatica*, 2006, 42(1):13-26.
- [12] Fu Minyue, Olbrot Andrzej W, Polis Michael P. Robust stability for time-delay systems: the edge theorem and graphical tests. *IEEE Transactions on Automatic Control*, Vol. 34, No. 8, pp 813-820, 1989.
- [13] Li Yinya, Sheng Andong, Wang Yuangang. Synthesis of PID-type controllers without parametric models: a graphical approach. *Energy Conversion and Management*, Vol. 49, No. 8, pp 2392-2402, 2008.
- [14] O Diekmann, van Gils, Verduyn Lunel. *Delay Equations : functional- , complex- and nonlinear analysis*. New York:Springer-Verlag, 1995.
- [15] Wang Dejin. A PID controller set of guaranteeing stability and gain and phase margins for time-delay systems. *Journal of Process Control*, Vol. 22, No. 7, pp 1298-1306, 2012.
- [16] Petr Husek. Decentralized PI controller design based on phase margin specifications. *IEEE Transactions on Control Systems Technology*, Vol. 22, No. 1, pp 346-351, 2014.

give permission, or have obtained permission from the copyright holder of this paper, for the publication and distribution of this paper as part of the ICAS proceedings or as individual off-prints from the proceedings.

Contact Author Email Address

liunan0530@163.com

Copyright Statement

The authors confirm that they, and/or their company or organization, hold copyright on all of the original material included in this paper. The authors also confirm that they have obtained permission, from the copyright holder of any third party material included in this paper, to publish it as part of their paper. The authors confirm that they